

High-resolution deep-sea carbon and oxygen isotope records of Eocene Thermal Maximum 2 and H2

Lucy Stap¹, Lucas J. Lourens¹, Ellen Thomas^{2,3}, Appy Sluijs⁴, Steven Bohaty⁵, and James C. Zachos⁶

¹Faculty of Geosciences, Utrecht University, 3584 CD Utrecht, Netherlands

²Department of Geology and Geophysics, Yale University, New Haven, Connecticut 06520, USA

³Department of Earth and Environmental Sciences, Wesleyan University, Middletown, Connecticut 06459, USA

⁴Biomarine Sciences, Institute of Environmental Biology, Utrecht University, 3584 CD Utrecht, Netherlands

⁵School of Ocean and Earth Science, National Oceanography Centre, University Road, Southampton SO17 1BJ, UK

⁶Earth and Planetary Sciences, University of California, Santa Cruz, California 95064, USA

ABSTRACT

Eocene Thermal Maximum 2 (ETM2) and H2 were two short-lived global warming events that occurred ~2 m.y. after the Paleocene–Eocene thermal maximum (PETM, ca. 56 Ma). We have generated benthic foraminiferal stable carbon and oxygen isotope records of four sites along a depth transect on Walvis Ridge (~3.5–1.5 km paleodepth, southeast Atlantic Ocean) and one site on Maud Rise (Weddell Sea) to constrain the pattern and magnitude of their carbon isotope excursions (CIEs) and deep-sea warming. At all sites, ETM2 is characterized by ~3 °C warming and a –1.4‰ CIE. The H2 event that occurred ~100 k.y. later is associated with ~2 °C warming and a –0.8‰ CIE. The magnitudes of the $\delta^{13}\text{C}$ and $\delta^{18}\text{O}$ excursions of both events are significantly smaller than those during the PETM, but their coherent relation indicates that the $\delta^{13}\text{C}$ change of the exogenic carbon pool was similarly related to warming during these events, despite the much more gradual and transitioned onset of ETM2 and H2.

INTRODUCTION

At least two prominent global warming events or hyperthermals were superimposed on the Late Paleocene through Early Eocene warming trend (ca. 60–50 Ma): the Paleocene–Eocene thermal maximum (PETM) at ca. 55.5 Ma (Kennett and Stott, 1991) and Eocene Thermal Maximum 2 (ETM2) at ca. 53.7 Ma (Lourens et al., 2005), also called H1 (Cramer et al., 2003). Both the PETM and ETM2 are marked by a pronounced negative carbon isotope excursion (CIE), recorded in both carbonate and organic carbon sedimentary components, and by a distinct carbonate dissolution horizon in deep-sea sediments, indicating the emission of large amounts ^{13}C -depleted carbon into the ocean-atmosphere system (Lourens et al., 2005; Zachos et al., 2005; Sluijs et al., 2009). The CIE of 1.0‰–1.5‰ in carbonate and ~3.5‰ in bulk organic matter and sea surface warming of ~3 °C during ETM2 were approximately half of those documented for the PETM (Lourens et al., 2005; Nicolo et al., 2007; McCarren et al., 2008; Sluijs et al., 2009; Stap et al., 2009). Along with the PETM and ETM2, a number of punctuated smaller negative $\delta^{13}\text{C}$ excursions (termed A to L) occurred during the Early Eocene, but the approximate magnitude of deep-sea warming during these events has not yet been established (Cramer et al., 2003; Nicolo et al., 2007). One of these events, H2, occurred ~100 k.y. after ETM2 and has a CIE of –0.2‰ to –0.7‰ in high-resolution bulk carbonate records from deep-sea and continental slope environments (Cramer et al., 2003; Nicolo et al., 2007; Stap et al., 2009).

Several possible explanations for the massive carbon input during the PETM have been proposed (Kurtz et al., 2003; Dickens et al., 1995; Svensen et al., 2004), and these may also hold for ETM2 (Lourens et al., 2005). However, an open issue is whether these events and other potential hyperthermals (such as H2) share a common origin. For example, an orbitally related mechanism may have triggered the injection of carbon from a similar source during the PETM, ETM2, and other short-lived $\delta^{13}\text{C}$ excursions (Cramer et al., 2003; Lourens et al., 2005; Westerhold et al., 2007). If so, the quantitative relation between changes in carbon flux and global temperature should be similar for these events, despite differences in magnitude. We assess this hypothesis by comparing high-resolution carbon and oxygen stable isotope records derived from benthic foraminiferal tests across ETM2 and H2 with published data for the PETM (McCarren et al., 2008; Thomas et al., 2002) obtained from the same deep-sea cores recovered by the Ocean Drilling Program in the southeast Atlantic Ocean and the Southern Ocean.

MATERIALS AND METHODS

High-resolution multispecimen $\delta^{13}\text{C}$ and $\delta^{18}\text{O}$ records of the benthic foraminiferal species *Nuttallides truempyi* were generated across ETM2 and H2 from four sites drilled over a 2 km depth transect with a paleodepth range of 1500–3600 m during Leg 208 along the Walvis Ridge (southeast Atlantic Ocean) (Zachos et al., 2004). Samples were taken from sites 1263, 1265, 1267, and 1262 at 0.5–1.0 cm resolution

through ETM2 and H2, and at 5–10 cm resolution in the interval below ETM2 and above H2. In addition, a single-specimen record was generated from site 690 in the Weddell Sea (Southern Ocean), with a paleodepth of ~1900 m (Thomas, 1990) (Fig. DR1 in the GSA Data Repository¹). From site 690, 83 samples were investigated, with an average sample resolution of ~5 cm. The H2 event is absent at site 690, due to an unconformity (Thomas, 1990; Cramer et al., 2003).

Within the Elmo horizon, i.e., the red clay layer that marks ETM2 at the Walvis Ridge sites, benthic foraminifera are small and thin-walled, and their species diversity is anomalously low. In the Elmo horizon of site 1263, *N. truempyi* is absent or very rare, so that no isotope data could be obtained for three samples (Fig. 1). We measured isotope ratios on *Oridorsalis umbonatus* from two of those samples, together with 24 samples from the ETM2 interval (Fig. DR4). No systematic offset was found between the $\delta^{18}\text{O}$ values of *N. truempyi* and *O. umbonatus*. Detailed scanning electron microscopy (SEM) images were conducted to see if the wall structure of *N. truempyi* is affected by diagenesis (Fig. DR2).

Prior to the analysis, all Walvis Ridge samples except for the small and thin-walled specimens (i.e., in total five samples from the Elmo clay layer of sites 1263 and 1265) were ultrasonically cleaned in methanol for 30 s, to remove adherent particulates. Stable isotope ratios were measured at Utrecht University using a CARBO-KIEL automated carbonate preparation device linked online to a Finnigan MAT253 mass spectrometer. Calibration to the international standard (NBS-19) and in-house standard (Naxos) revealed an analytical 1σ precision better than 0.02‰ and 0.08‰ for $\delta^{13}\text{C}$ and $\delta^{18}\text{O}$, respectively. Replicate measurements on ~7% of the samples indicate mean reproducibility better than 0.08‰ for $\delta^{13}\text{C}$ and $\delta^{18}\text{O}$. All values are reported in standard delta notation (δ) relative to VPDB (Vienna Peedee belemnite). Data

¹GSA Data Repository item 2010166, Figures DR1–DR5, is available online at www.geosociety.org/pubs/ft2010.htm, or on request from editing@geosociety.org or Documents Secretary, GSA, P.O. Box 9140, Boulder, CO 80301, USA.

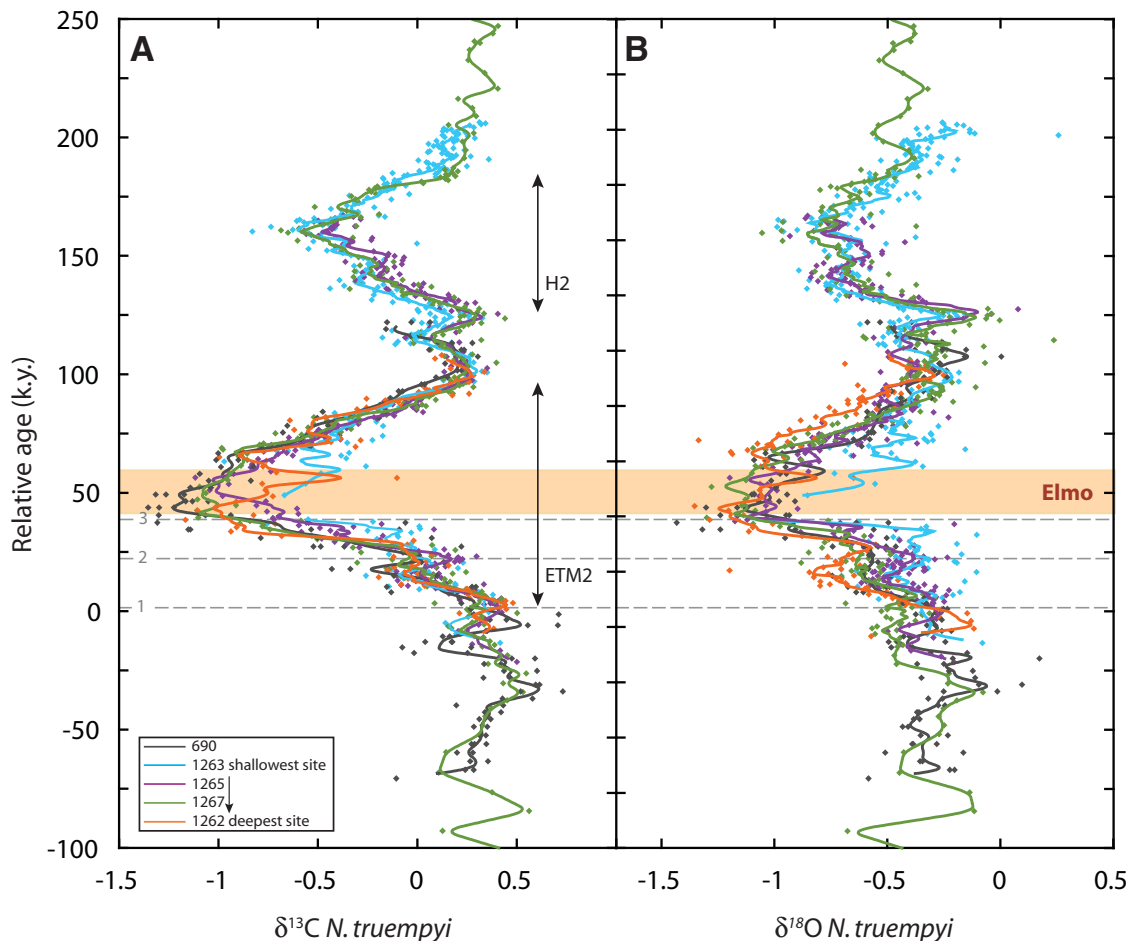


Figure 1. Relative age during ETM2 and H2 for sites 1263, 1265, 1267, 1262, and 690 plotted versus benthic foraminiferal carbon (A) and oxygen (B) isotope records of *Nuttallides truempyi*. Lines represent 4 k.y. moving average. The relative age model for ETM2 and H2 is based on changes in CaCO_3 wt% and the assumption of a close to constant terrigenous input flux over time (Stap et al., 2009). Benthic isotope data of site 690 are plotted against the relative age model of all Walvis Ridge sites using the Match program (Lisiecki and Lisiecki, 2002). Site 690 data against depth are shown in Fig. DR3 (in the Data Repository [see footnote 1]). Dashed gray lines indicate the $\delta^{13}\text{C}$ transitions during the onset of ETM2 according to Stap et al. (2009). Indicated in light orange is the Elmo horizon (Lourens et al., 2005).

are plotted on the relative age model of Stap et al. (2009), which is based on assuming a constant terrigenous sediment flux and a duration of 100 k.y. between the clay layers associated with ETM2 (i.e., Elmo) and H2.

RESULTS AND DISCUSSION

ETM2 and H2 are characterized by pronounced and concomitant negative $\delta^{13}\text{C}$ (respectively -1.4‰ and -0.8‰) and $\delta^{18}\text{O}$ (respectively -0.8‰ and -0.5‰) excursions at intermediate to abyssal water depths (Fig. 1). The $\delta^{13}\text{C}$ and $\delta^{18}\text{O}$ excursions during ETM2 are less pronounced at site 1263 than at the other sites. A similar pattern is depicted in the isotope records of the benthic foraminifera *Anomalinoidea* spp. (Lourens et al., 2005) and *O. umbonatus* (Fig. DR4). Benthic foraminiferal abundances in the Elmo horizon are exceptionally low, possibly due to an expansion of the oxygen minimum zone, which excluded many species of benthic foraminifera and all large specimens from the relatively shallow depths (site 1263) during the nadir of the excursion. This, combined with bioturbation, may have biased the multispecimen record at this site.

In addition, scanning electron micrographs revealed that the wall structure of *N. truempyi*

is moderately altered by recrystallization and/or secondary calcite throughout the studied interval of all sites (Fig. DR2). We therefore suspect that a larger diagenetic overprint of the primary isotopic signal at the shallower Walvis Ridge sites caused the on-average heavier $\delta^{18}\text{O}$ values, in particular within ETM2 (Fig. 1).

In general, the oxygen (and carbon) isotopic compositions of benthic foraminifera in deep-sea cores are thought to be less altered by early diagenesis than those of planktic foraminifera (Sexton et al., 2006) and therefore can be used to estimate deep-sea temperatures. The mean $\delta^{18}\text{O}$ values of the studied sites prior to ETM2 are -0.1‰ to -0.3‰ (Fig. 1), indicating a deep-sea temperature of $\sim 12\text{ °C}$ (Bemis et al., 1998), consistent with the global benthic stack for this time interval (Zachos et al., 2001). The $\sim 0.8\text{‰}$ drop in $\delta^{18}\text{O}$ values during ETM2 implies that deep-sea temperatures rose by $>3\text{ °C}$ to peak temperatures of $15\text{--}16\text{ °C}$. Single-specimen-derived temperatures at site 690 are very similar (Fig. 1), indicating interregional consistency and thus a uniform magnitude of deep-sea warming at these locations and depths during ETM2. The $\delta^{18}\text{O}$ decrease of $\sim 0.5\text{‰}$ associated with H2 shows that deepwater temperatures increased by as much as $\sim 2\text{ °C}$ (e.g., from ~ 12 to 14 °C).

The uniformity between the $\delta^{13}\text{C}$ and $\delta^{18}\text{O}$ trends and absolute values for ETM2 and H2 among the different Walvis Ridge sites suggests that the deep-sea water column was homogeneous during the Early Eocene. This observation supports previous inferences from data and modeling studies (Emanuel, 2002; Via and Thomas, 2006) that point to a different structure of the oceans and circulation mode during the early Paleogene than today, i.e., with reduced meridional surface temperature and vertical temperature gradients (e.g., Zachos et al., 1992; Bijl et al., 2009). Site 690 in the Southern Ocean reveals essentially the same $\delta^{13}\text{C}$ and $\delta^{18}\text{O}$ patterns and values as the Walvis Ridge sites, suggesting that they were all bathed by a water mass of similar temperature and dissolved inorganic carbon (DIC) isotopic content ($\delta^{13}\text{C}_{\text{DIC}}$), probably a single Southern Ocean intermediate to deep water mass (Via and Thomas, 2006).

The onsets of ETM2 and H2 are characterized by multiple transitions in $\delta^{13}\text{C}$ and $\delta^{18}\text{O}$ (Fig. 1), which covary with the precession-paced steps in bulk carbonate isotope records and carbonate dissolution reported in Stap et al. (2009). From the onset of ETM2 at a relative age of 0 k.y., $\delta^{13}\text{C}$ and $\delta^{18}\text{O}$ values dropped by respectively $\sim 1.4\text{‰}$ and $\sim 0.8\text{‰}$ along two major transitions

(Fig. 1). The largest excursion in the benthic $\delta^{18}\text{O}$ and $\delta^{13}\text{C}$ records occurred during transition 2 of ETM2 (i.e., between 21 and 40 k.y. after the onset). Transition 3, which coincides with the base of the Elmo horizon (i.e., interval of maximum carbonate dissolution) (Stap et al., 2009), is not marked by a significant shift in benthic $\delta^{18}\text{O}$ and $\delta^{13}\text{C}$ values. Remarkably, in contrast to carbonate dissolution patterns (Stap et al., 2009), the recovery phases of the isotope records lack the precession-paced shifts of Stap et al. (2009), suggesting a partial decoupling between changes in deep-sea $\delta^{13}\text{C}_{\text{DIC}}$ and carbonate saturation state during this period.

To assess whether ETM2 shares characteristics with the PETM in terms of carbon cycle and climate, we compared the covariance of benthic foraminiferal $\delta^{13}\text{C}$ and $\delta^{18}\text{O}$ values. For ETM2 (including transitions 1 and 2) and H2, $\Delta\delta^{18}\text{O}/\Delta\delta^{13}\text{C}$ is roughly 0.8/1.4 and 0.5/0.8, respectively (Figs. 1 and 2). Remarkably, the PETM $\delta^{13}\text{C}$ and $\delta^{18}\text{O}$ excursions in *N. truempyi* and *O. umbonatus* of -3.5‰ and -2.4‰ at site 1263 (McCarren et al., 2008) reveal an almost iden-

tical relation with a slope of 0.69, regardless of their much larger magnitudes (Fig. 2). The coherent relationship in benthic $\delta^{13}\text{C}$ and $\delta^{18}\text{O}$ indicates that the $\delta^{13}\text{C}$ change of the exogenic carbon pool was similarly related to warming during the PETM, ETM2, and H2. Assuming that climate sensitivity did not change significantly during the Early Eocene, this suggests that the isotopic composition of the source(s) of carbon was similar for these events, as suggested previously (Lourens et al., 2005; Nicolo et al., 2007). This can be tested by using the carbonate dissolution horizons to constrain the total mass of carbon released during ETM2 as has been done for the PETM (Ridgwell, 2007; Zeebe et al., 2009). One complicating factor in comparing the $\delta^{13}\text{C}$, temperature, and deep-sea carbonate dissolution records for the PETM, ETM2, and H2 is that the latter two events apparently had a much more gradual onset. In particular, several single specimens from the onset of ETM2 at site 690 show $\delta^{13}\text{C}$ and $\delta^{18}\text{O}$ values that seem intermediate between the pre-ETM2 and minimum ETM2 data populations

(Figs. 1 and DR3). Such intermediate values have not been observed in any PETM section (Thomas et al., 2002; Zachos et al., 2007), even at locations with much higher sedimentation rates (John et al., 2008), though with less robust age control. All available information, hence, suggests that a significant portion of the carbon injection during the PETM occurred in less than 10 k.y., while the entire carbon injection during ETM2 took ~ 20 k.y. with the current age model at Walvis Ridge (from transition 2 onwards in Fig. 1). Regardless of the apparently different rate of carbon injection during the events, the data imply that the change in global exogenic $\delta^{13}\text{C}$ was similarly proportional to the degree of warming during the PETM, ETM2, and H2.

ACKNOWLEDGMENTS

We are grateful to Gerald R. Dickens and two anonymous reviewers for their constructive comments. This research used samples provided by the Integrated Ocean Drilling Program (IODP). Funding for this research was provided by the Darwin Center for Biogeosciences to Lourens, Sluijs, and Stap, by the Netherlands Organisation for Scientific Research

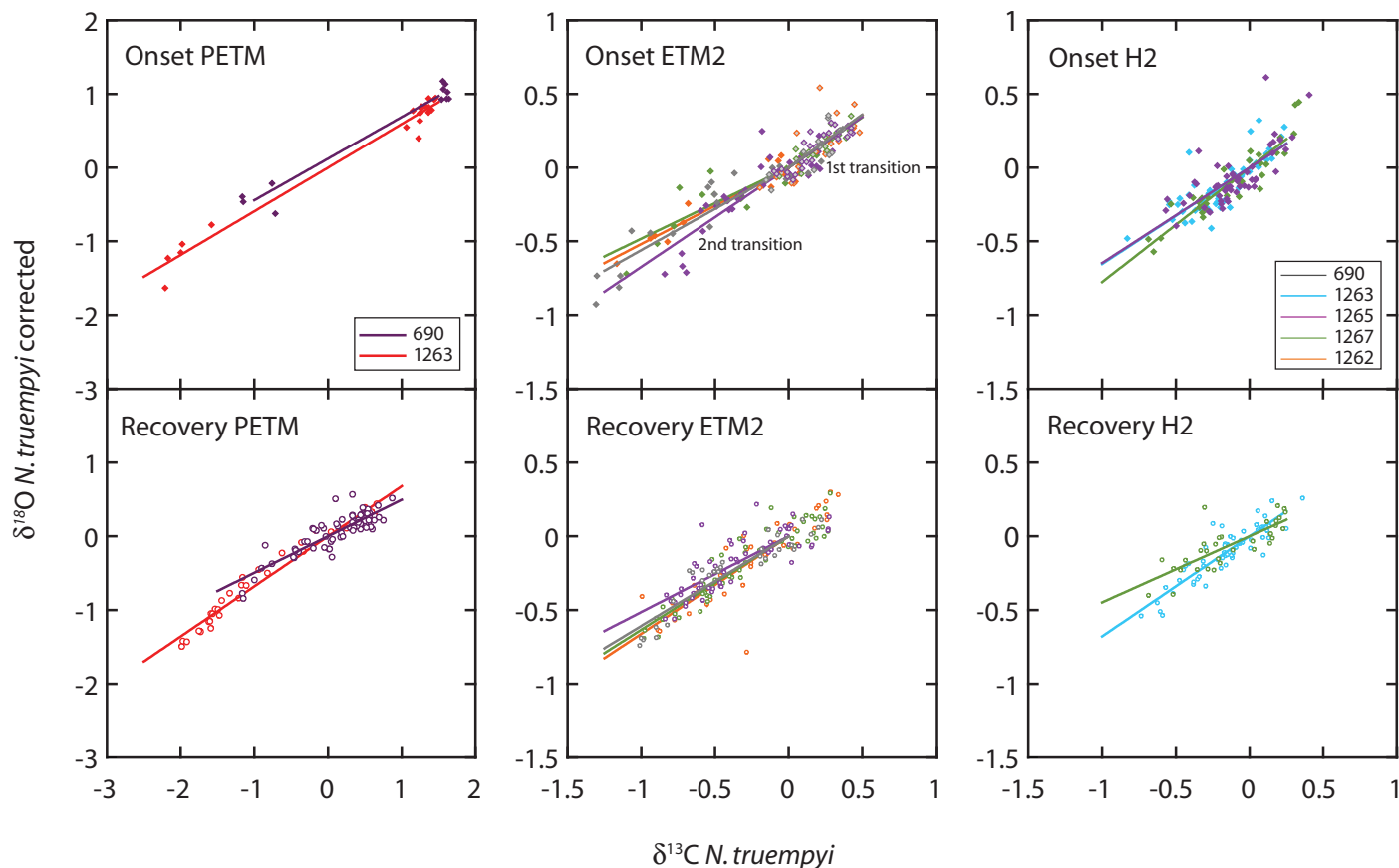


Figure 2. Relationship between the oxygen and carbon isotope values of *Nuttallides truempyi* during the onset and recovery of ETM2, H2, and PETM. Comparison between PETM multispecimen data derived from sites 1263 and 690 (Kennett and Stott, 1991; Thomas et al., 2002; McCarren et al., 2008) and ETM2 (this study). Note that, because of severe carbonate dissolution and/or the absence of comparable taxa during the onset of the PETM (Thomas et al., 2000; McCarren et al., 2008), only the first four CIE values are taken from site 690. For ETM2 the relationship between the oxygen and carbon isotope values of 1st (0–14 k.y.) and 2nd (21–40 k.y.) transition and recovery (60–100 k.y.) are shown. The scales of the $\delta^{13}\text{C}$ and $\delta^{18}\text{O}$ axes for ETM2 and H2 are half those of the PETM.

to Lourens (ALW investments grant 834.04.003) and Sluijs (Veni grant 863.07.001), and by National Science Foundation grants EAR-010727 and EAR-0628719 to Thomas and Zachos. We thank A. van Dijk, M. Ziegler, and G. Ittman for technical support, and Karolina Koho and Tanja Kouwenhoven for making the SEM photographs. This is publication number DW-2009-5003 of the Darwin Center for Biogeosciences.

REFERENCES CITED

- Bemis, B.E., Spero, H.J., Bijma, J., and Lea, D.W., 1998, Reevaluation of the oxygen isotopic composition of planktonic foraminifera: Experimental results and revised paleotemperature equations: *Paleoceanography*, v. 13, p. 150–160, doi: 10.1029/98PA00070.
- Bijl, P.K., Schouten, S., Sluijs, A., Reichert, G.-J., Zachos, J.C., and Brinkhuis, H., 2009, Early Palaeogene temperature evolution of the southwest Pacific Ocean: *Nature*, v. 461, p. 776–779, doi: 10.1038/nature08399.
- Cramer, B.S., Wright, J.D., Kent, D.V., and Aubry, M.-P., 2003, Orbital climate forcing of $\delta^{13}\text{C}$ excursions in the late Paleocene–early Eocene (chrons C24n–C25n): *Paleoceanography*, v. 18, p. 1097, doi: 10.1029/2003PA000909.
- Dickens, G.R., O’Neil, J.R., Rea, D.K., and Owen, R.M., 1995, Dissociation of oceanic methane hydrate as a cause of the carbon isotope excursion at the end of the Paleocene: *Paleoceanography*, v. 10, p. 965–971, doi: 10.1029/95PA02087.
- Emanuel, K., 2002, A simple model of multiple climate regimes: *Journal of Geophysical Research (Atmospheres)*, v. 107, 4077, doi: 10.1029/2001JD001002.
- John, C.M., Bohaty, S.M., Zachos, J.C., Sluijs, A., Gibbs, S.J., Brinkhuis, H., and Bralower, T.J., 2008, North American continental margin records of the Paleocene–Eocene thermal maximum: Implications for global carbon and hydrological cycling: *Paleoceanography*, v. 23, PA2217, doi: 10.1029/2007PA001465.
- Kennett, J.P., and Stott, L.D., 1991, Abrupt deep-sea warming, palaeoceanographic changes and benthic extinctions at the end of the Paleocene: *Nature*, v. 353, p. 225–229, doi: 10.1038/353225a0.
- Kurtz, A.C., Kump, L.R., Arthur, M.A., Zachos, J.C., and Paytan, A., 2003, Early Cenozoic decoupling of the global carbon and sulfur cycles: *Paleoceanography*, v. 18, 1090, doi: 10.1029/2003PA000908.
- Lisiecki, L.E., and Lisiecki, P.A., 2002, Application of dynamic programming to the correlation of paleoclimate records: *Paleoceanography*, v. 17, p. 1049, doi: 10.1029/2001PA000733.
- Lourens, L.J., Sluijs, A., Kroon, D., Zachos, J.C., Thomas, E., Röhl, U., Bowles, J., and Raffi, I., 2005, Astronomical pacing of late Palaeocene to early Eocene global warming events: *Nature*, v. 435, p. 1083–1087, doi: 10.1038/nature03814.
- McCarren, H., Thomas, E., and Hasegawa, T., Röhl, U., and Zachos, J.C., 2008, Depth dependency of the Paleocene–Eocene carbon isotope excursion: Paired benthic and terrestrial biomarker records (Ocean Drilling Program Leg 208, Walvis Ridge): *Geochemistry, Geophysics, Geosystems*, v. 9, Q10008, doi: 10.1029/2008GC002116.
- Nicolo, M.J., Dickens, G.R., Hollis, C.J., and Zachos, J.C., 2007, Multiple early Eocene hyperthermals: Their sedimentary expression on the New Zealand continental margin and in the deep sea: *Geology*, v. 35, p. 699–702, doi: 10.1130/G23648A.1.
- Ridgwell, A., 2007, Interpreting transient carbonate compensation depth changes by marine sediment core modeling: *Paleoceanography*, v. 22, PA4102, doi: 10.1029/2006PA001372.
- Sexton, P.F., Wilson, P.A., and Pearson, P.N., 2006, Microstructural and geochemical perspectives on planktic foraminiferal preservation: “Glassy” versus “Frosty”: *Geochemistry, Geophysics, Geosystems*, v. 7, Q12P19, doi: 10.1029/2006GC001291.
- Sluijs, A., Schouten, S., Donders, T.H., Schoon, P.L., Röhl, U., Reichert, G.-J., Sangiorgi, F., Kim, J.-H., Sinnighe Damste, J.S., and Brinkhuis, H., 2009, Warm and wet conditions in the Arctic region during Eocene Thermal Maximum 2: *Nature Geoscience*, v. 2, p. 777–780, doi: 10.1038/ngeo668.
- Stap, L., Sluijs, A., Thomas, E., and Lourens, L., 2009, Patterns and magnitude of deep sea carbonate dissolution during Eocene Thermal Maximum 2 and H2, Walvis Ridge, southeastern Atlantic Ocean: *Paleoceanography*, v. 24, PA1211, doi: 10.1029/2008PA001655.
- Svensen, H., Planke, S., Mørner, S., Jamveit, B., Myklebust, R., Eidem, T.R., and Rey, S.S., 2004, Release of methane from a volcanic basin as a mechanism for initial Eocene global warming: *Nature*, v. 429, p. 542–545, doi: 10.1038/nature02566.
- Thomas, D.J., Zachos, J.C., Bralower, T.J., Thomas, E., and Bohaty, S., 2002, Warming the fuel for the fire: Evidence for the thermal dissociation of methane hydrate during the Paleocene–Eocene thermal maximum: *Geology*, v. 30, p. 1067–1070, doi: 10.1130/0091-7613(2002)030<1067:WTF>2.0.CO;2.
- Thomas, E., 1990, Late Cretaceous through Neogene deep-sea benthic foraminifera (Maud Rise, Weddell Sea, Antarctica): *Proceedings of the Ocean Drilling Program, Scientific results, ODP Leg 113, Weddell Sea, Antarctica*, p. 571–594.
- Thomas, E., Zachos, J.C., and Bralower, T.J., 2000, Deep-Sea Environments on a Warm Earth: Latest Paleocene–early Eocene, *in* Huber, B.T., Macleod, K.G., and Wing, S.L., eds., *Warm Climates in Earth History*: Cambridge, Cambridge University Press, p. 132–160.
- Via, R.K., and Thomas, D.J., 2006, Evolution of Atlantic thermohaline circulation: Early Oligocene onset of deep-water production in the North Atlantic: *Geology*, v. 34, p. 441–444, doi: 10.1130/G22545.1.
- Westerhold, T., Röhl, U., Laskar, J., Raffi, I., Bowles, J., Lourens, L.J., and Zachos, J.C., 2007, On the duration of magnetochrons C24r and C25n and the timing of early Eocene global warming events: Implications from the Ocean Drilling Program Leg 208 Walvis Ridge depth transect: *Paleoceanography*, v. 22, PA2201, doi: 10.1029/2006PA001322.
- Zachos, J.C., Rea, D.K., Seto, K., Niitsuma, N., and Nomura, N., 1992, Paleogene and early Neogene deep water history of the Indian Ocean: Inferences from stable isotopic records, *in* Duncan, R.A., et al., eds., *The Indian Ocean: A synthesis of results from the Ocean Drilling Program: American Geophysical Union Geophysical Monograph 70*, p. 351–386.
- Zachos, J.C., Pagani, M., Sloan, L., Thomas, E., and Billups, K., 2001, Trends, rhythms, and aberrations in global climate 65 Ma to present: *Science*, v. 292, p. 686–693, doi: 10.1126/science.1059412.
- Zachos, J.C., and 27 others, 2004, *Proceedings of the Ocean Drilling Program, Initial Reports, Volume 208: College Station, Texas, Ocean Drilling Program*, p. 1–112.
- Zachos, J.C., Röhl, U., Schellenberg, S.A., Sluijs, A., Hodel, D.A., Kelly, D.C., Thomas, E., Nicolo, M., Raffi, I., Lourens, L.J., McCarren, H., and Kroon, D., 2005, Rapid acidification of the ocean during the Paleocene–Eocene thermal maximum: *Science*, v. 308, p. 1611–1615, doi: 10.1126/science.1109004.
- Zachos, J.C., Bohaty, S., John, C., and McCarren, H., 2007, The Paleocene–Eocene carbon isotope excursion: Constraints from individual shell planktonic foraminifer records: *Royal Society of London Philosophical Transactions, ser. A*, v. 365, p. 1829–1842, doi: 10.1098/rsta.2007.2045.
- Zeebe, R.E., Zachos, J.C., and Dickens, G.R., 2009, Carbon dioxide forcing alone insufficient to explain Palaeocene–Eocene Thermal Maximum warming: *Nature Geoscience*, v. 2, p. 576–580, doi: 10.1038/NNGEO578.

Manuscript received 14 October 2009

Revised manuscript received 4 January 2010

Manuscript accepted 2 February 2010

Printed in USA